Biol. Chem., Vol. 382, pp. 1271 – 1276, August 2001 · Copyright © by Walter de Gruyter · Berlin · New York

Photo-CIDNP ^{13}C Magic Angle Spinning NMR on Bacterial Reaction Centres: Exploring the Electronic Structure of the Special Pair and Its Surroundings

Jörg Matysik[1,*], Els Schulten[1], Alia[1,2], Peter Gast[2], Jan Raap[1], Johan Lugtenburg[1], Arnold J. Hoff[2] and Huub J. M. de Groot[1,*]

[1] Leiden Institute of Chemistry, Gorlaeus Laboratoria, P.O. Box 9502, NL-2300 RA Leiden, The Netherlands
[2] Department of Biophysics, Huygens Laboratory, P.O. Box 9504, NL-2300 RA Leiden, The Netherlands

* Corresponding authors

Photochemically induced dynamic nuclear polarisation (photo-CIDNP) in intact bacterial reaction centres has been observed by ^{13}C-solid state NMR under continuous illumination with white light. Strong intensity enhancement of ^{13}C NMR signals of the aromatic rings allows probing the electronic ground state of the two BChl cofactors of the special pair at the molecular scale with atomic selectivity. Differences between the two BChl cofactors are discussed. Several aliphatic ^{13}C atoms of cofactors, as well as ^{13}C atoms of the imidazole ring of histidine residue(s), show nuclear-spin polarisation to the same extent as the aromatic nuclei of the cofactors. Mechanisms and applications of polarisation transfer are discussed.
Key words: Chlorophyll / Histidine / Photo-CIDNP / Photosynthesis / Solid-state NMR.

Introduction

Conversion of light to chemical energy in photosynthesis is associated with charge separation across photosynthetic membranes. In photosynthetic reaction centres of purple bacteria, a complex chain of electron transfer reactions is initiated by ejection of an electron from the excited, strongly coupled bacteriochlorophyll *a* (BChl *a*) dimer, the 'special pair' (P). Upon photo-excitation into its first electronically excited singlet state, P* transfers within 3 ps an electron to the primary acceptor, a bacteriopheophytin (BPhe) molecule. In a next step an electron is transferred from BPhe to the primary quinone acceptor Q_A in about 200 ps. Subsequently, in a much slower reaction, taking about 100 μs, an electron is transferred from Q_A to the final electron acceptor Q_B. This light-induced electron transfer sequence is repeated after the special pair has been re-reduced by a cytochrome. Although both the spatial structure and the electron transfer kinetics of several RCs are described in great detail, there is no clear understanding of the mechanism by which electron emission from the electronically excited primary electron donor occurs. In addition, a detailed picture of the molecular mechanism of the inhibition of the back reaction, which is probably due to a high exothermic reaction enthalpy pushing the system into the inverted Marcus region (Bixon *et al*., 1993), is missing. To address these questions, we aim at resolving details of the functionally crucial electronic structure of transient species in the electron transfer process with atomic selectivity using spectroscopic methods.

The triplet quantum yield of the light-induced electron transfer in quinone-blocked RCs depends on the strength of the applied magnetic field. This magnetic field effect has been qualitatively interpreted in terms of nuclear couplings affecting the mixing rate of the radical pair (Blankenship *et al.*, 1977; Hoff *et al.*, 1977b). Polarisation of the electrons in the electron pair interacting with nuclei has been observed by EPR spectroscopy (Hoff *et al*., 1977a; for reviews, see Hoff, 1981, 1984). The corresponding spin polarisation of the nuclei can be observed by NMR spectroscopy *via* the photochemically induced dynamic nuclear polarisation (photo-CIDNP). Photo-CIDNP is well known from liquid NMR (for a review, see Hore and Broadhurst, 1993). A reaction mechanism providing photo-CIDNP in liquids has been described in terms of a radical-pair mechanism (Kaptein, 1975, 1977). Photosynthetic RCs are, however, too large to be investigated by liquid NMR. The application of Magic Angle Spinning (MAS) solid-state NMR spectroscopy allows the observation of photo-CIDNP in frozen samples of bacterial reaction centres (Zysmilich and McDermott, 1994a, b, 1996; Matysik *et al*., 2000a, 2001) and of plant reaction centres (Matysik *et al.*, 2000b). The observation of light-induced nuclear polarisation in the solid state is possible since the relaxation time for nuclei is much longer than for electrons. Jeschke (1997, 1998) proposed an electron-electron-nuclear three-spin mixing interaction mechanism to explain the earlier photo-CIDNP observations. In this scheme a spin-correlated radical pair polarises nuclei with Zeeman frequencies close to the matching condition corresponding with the difference of the Zeeman energies of the two electrons. In that case, sign and intensity of the photo-CIDNP signal would be related to the electron-spin density localised at the particular nucleus. Nuclear coherences caused by the sudden photo-generation of the spin-correlated radical pair have been indeed observed by time-resolved EPR spectroscopy (Weber *et*

al., 1996; Kothe *et al.*, 1998). Sorting of nuclear spins can occur by the very fast recombination of the triplet radical pair, since the molecular triplet has left the electron-electron-nuclear three-spin system (Polenova and McDermott, 1999). Additional polarisation may be obtained by the different nuclear relaxation kinetics of the singlet and paramagnetic triplet species (McDermott *et al*., 1998). A triplet mechanism is unlikely since signals from the BPheo are observed with high intensity (Zysmilich and McDermott, 1994, 1996b; Schulten *et al*., unpublished). Alternative mechanisms for solid-state photo-CIDNP have been examined by van den Heuvel *et al.* (1994) and Corvaja *et al.* (2000). A similar discussion of the photo-CIDNP effect observed with liquid NMR for rigid organic systems has been discussed by Wegner *et al.* (1999, 2001).

The strong enhancement of the NMR lines from photochemically active regions in the RC protein complex provides a window on the ground-state electronic structure and its changes during the electron transfer events on the atomic level. The application of photo-CIDNP in conjunction with selective isotope labelling is particularly powerful since it combines two methods for enhancing intensity and selectivity. In addition, these experiments can help to elucidate the mechanisms of how nuclear polarisation is established by the electron transfer. Here we report some recent photo-CIDNP data collected from natural abundance and selectively ^{13}C-labelled *Rhodobacter sphaeroides* RCs. Their implications for understanding the mechanisms of charge separation and photo-CIDNP are discussed.

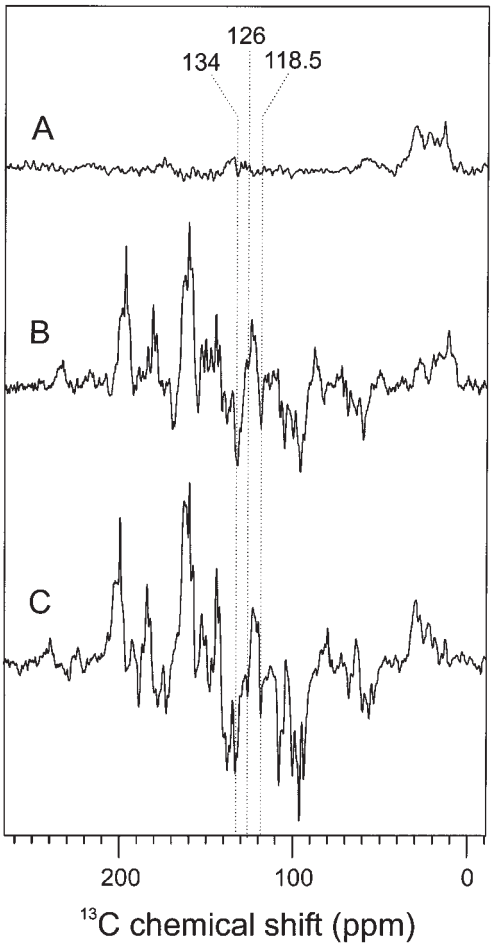

Fig. 1 ^{13}C MAS NMR Spectra of Natural Abundance Quinone-Depleted Reaction Centres of *R. sphaeroides* R-26.
The spectra were acquired at 220 K in the dark (A) and using continuous illumination with white light (B,C). The spinning frequency around the magic angle was 3.6 kHz for the spectrum B, and 4 kHz for the spectra A and C.

Results and Discussion

Photo-CIDNP in Natural Abundance Reaction Centres

Figure 1A shows the ^{13}C-MAS NMR spectrum of the natural abundance ^{13}C in a sample of quinone-depleted reaction centres of *R. sphaeroides* R26. The data were acquired with a spinning frequency of 4.0 kHz in the dark at a temperature of 220 K. The aliphatic response between 10 and 50 ppm is mainly from the apoprotein. The aromatic and olefinic signals between 110 and 140 ppm, and the carbonyl signals around 170 ppm are very weak. With continuous illumination, strong ^{13}C NMR signals from spin-polarised nuclei are observed (Figure 1B and C). Carbon nuclei in the aromatic ring systems involved in the photochemistry are enhanced by the photo-CIDNP. Both enhanced-absorptive (positive) and emissive (negative) ^{13}C NMR lines appear in the photo-CIDNP spectrum. Several emissive signals (110.5, 106.8, 101.5, 97.8 and 95.8 ppm) are detected in the region of the methine response of BChl *a* cofactors. Only signals in the aromatic region are enhanced by photo-CIDNP, whereas no enhancement can be observed in the region of aliphatic carbons. The data shown in Figure 1B,C are similar to the results obtained for dense pellets of the same biological system (Zysmilich and McDermott, 1996a). It is remarkable that the emissive signals of the methine carbons have very similar intensities. This indicates a rather homogeneous electron spin density distribution within the macrocycles in the radical cation state, and is different from the asymmetric electron spin density pattern observed in photosystem II (Matysik *et al*., 2000b). Many of the signals appear unresolved. Since more than four negative signals from methine carbons are observed at least two different cofactor species are involved in photo-CIDNP. To distinguish centrebands from sidebands, data sets with different MAS frequencies of 3.6 and 4 kHz were acquired (Figure 1B, C). In addition, it has been shown that it is impossible to assign all signals to a single BChl molecule (Matysik *et al*., 2001). This provides evidence that the photo-CIDNP response is composed of a complicated pattern of strongly overlapping absorptive and emissive centre- and sidebands from more than just a single BChl *a* cofactor of the special pair as suggested earlier (Zysmilich and McDermott, 1996a).

The Involvement of Magnesium-Bound Histidine

The reaction centres of *R. sphaeroides* contain 20 histidine residues. Histidine 173 of chain L and histidine 202 of chain M coordinate with the magnesium of the special pair (P). Similarly, histidine 153 of chain L and histidine 182 of chain M are coordinated with the magnesium of the accessory bacteriochlorophylls (Deisenhofer *et al*., 1985). Zysmilich and McDermott (1994, 1996b) have shown that signals from one or more histidine residues can be detected in ^{15}N photo-CIDNP data from reaction centres of *R. sphaeroides*. These ^{15}N signals are emissive with similar intensity as the ^{15}N signals from the cofactors. Hence, an observation of ^{13}C photo-CIDNP NMR signals from histidine side chains should then also be possible in a natural abundance sample. Very recently, the ^{13}C chemical shifts of a magnesium-coordinating histidine side chain have been measured at 117 (δ-C), 135 (ε-C) and 125 ppm (γ-C) (Alia *et al*., 2001) (see Figure 2 for nomenclature). The spectra in Figure 1B and C clearly show negative signals at 118.5 and 134.0 ppm. The intensity is on the same order of magnitude as the intensity of the emissive signals arising from the methine carbons. This leads us to assign these signals to the δ- and ε-C atoms of a magnesium-bound histidine, probably the axial ligand of a BChl *a* cofactor. A signal that can be attributed to the γ-C, on the imidazole ring remote from the magnesium-bound nitrogen, appears to be much weaker. The negative signals at 118.5 and 134.0 ppm have not been discussed in the earlier work (Zysmilich and McDermott, 1996a; Matysik *et al.*, 2000a). This can be due to lower spectral quality. To investigate whether the increase of negative signals compared to the positive signals is caused by a stronger light intensity will be of high interest in order to resolve the mechanism of photo-CIDNP in the solid state.

The Electronic Structure of the Special Pair

Selective isotope labelling provides an excellent opportunity to improve both the selectivity and the sensitivity of the photo-CIDNP NMR experiment. In addition, two-dimensional photo-CIDNP dipolar correlation spectroscopy can be performed, providing an unambiguous assignment of the label response and a MAS NMR chemical shift image of the electronic structure of photochemically active parts at the atomic scale. Figure 3 shows a [1,3,6,8,11,13,17,19-$^{13}C_8$]-BChl molecule. RC preparations with this labeling pattern in all BChl and BPhe cofactors were investigated by MAS NMR (Figure 4). Spectrum

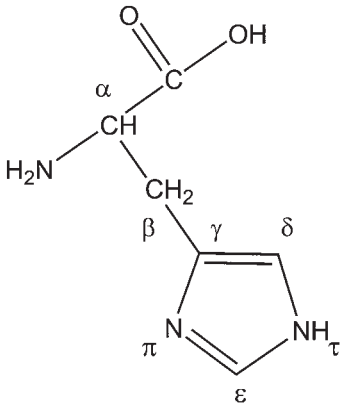

Fig. 2 The Chemical Structure and IUPAC Numbering Scheme of Histidine.

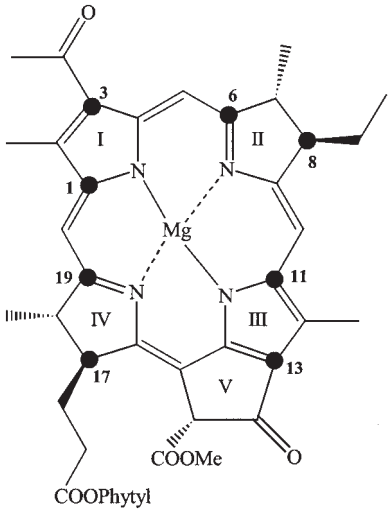

Fig. 3 Structure of a [1,3,6,8,11,13,17,19-$^{13}C_8$]-BChl Molecule. The labelled positions are indicated with filled circles.

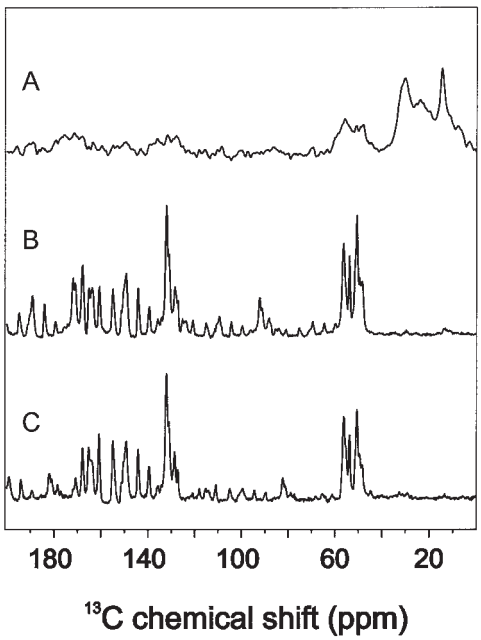

Fig. 4 ^{13}C MAS NMR Spectrum of Quinone-Reduced [1,3,6,8,11,13,17,19-$^{13}C_8$]-BChl/BPhe Labelled Bacterial RC.
(A) Spectrum acquired in the dark with a spinning frequency 4 kHz. Spectra (B) and (C) were measured using continuous illumination with white light and spinning frequencies of 4 kHz (B) and 5 kHz (C).

A in Figure 4 was recorded for two days with Hartmann-Hahn cross polarisation in the dark. Broad weak responses from the labelled carbon atoms can be identified in the aliphatic and the aromatic regions. Upon illumination, strong signals appear at these positions. Spectra 4B and C have been collected within 60 minutes. In the light the strongest natural abundance signal at 15 ppm is barely visible and can be used as an internal marker to quantify the enhancement of the signal due to the photo-CIDNP. While in the dark spectrum the signal has 2.5 times the intensity of the signal at 54 ppm of a labelled carbon atom, with illumination the signal at 54 ppm is approximately 35 times stronger than the signal at 15 ppm. Considering that the signal at 54 ppm in the dark spectrum is probably associated with the signals from two cofactors superimposed on a background of the apoprotein, a rough estimate of the enhancement factor due to the photo-CIDNP effect of 200 to 300 is obtained for this experiment. Experiments at different spinning frequencies (Figure 4B and C) allow the identification of the centrebands. In a deconvolution procedure with Lorentz functions, individual photo-CIDNP signals were extracted (Figure 5). Based on the chemical shifts, the response is assigned to two BChl, probably of P, and the BPhe of the photochemically active branch. The deconvolution shows that the chemical shift differences between BChl molecules are significant. Therefore, these data provide evidence that the two BChl molecules of P are already electronically distinguished in the electronic ground state. It is thus clear that photo-CIDNP can yield information about the electronic structure of the ground state of the photochemically active BChls in P at atomic resolution. A more detailed study, providing clear assignments by 2-dimensional photo-CIDNP experiments will be published soon (Schulten *et al*., in preparation).

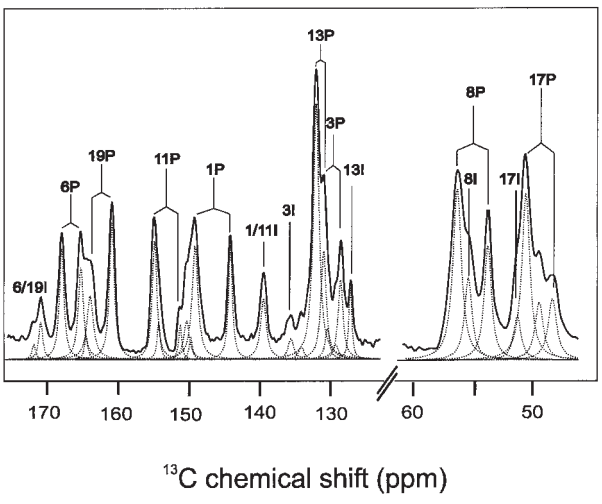

Fig. 5 Detailed View on the ^{13}C-MAS NMR Spectrum of Figure 4C, Fitted with Lorentz Functions.
Signals labelled with 'P' and 'I' are assigned to BChl and BPhe, respectively.

The Involvement of Aliphatic Atoms of the BChl Macrocycle

The HOMO is expected to contain the unpaired electron-spin density and this molecular orbital should reside predominantly in the aromatic system. Hence, the natural abundance sample does not show signal enhancement in the aliphatic region (Figure 1). Under natural abundance conditions, the probability to find two ^{13}C atoms close to each other is very low. Therefore, no transfer of polarisation to the aliphatic carbons can occur. In the selective isotope-labelled sample the aliphatic carbons show enhancement comparable to the aromatic carbons (Figure 4). At this ^{13}C-label concentration, aliphatic ^{13}C atoms can be polarised by neighbouring aromatic ^{13}C atoms. Therefore, in selectively isotope-labelled samples, the transfer of nuclear polarisation provides a tool to study also the ground state electronic structure of atoms in the neighbourhood of the aromatic system. On the other hand, at high isotope label concentrations, fast dissipation of nuclear polarisation into the bath of interacting nuclear spins destroys all nuclear polarisation. This appears to be the reason for the absence of polarisation in the ^{1}H spectrum (Zysmilich and McDermott, 1996a) and in the ^{13}C spectrum of uniformly ^{13}C-labelled bacterial RCs (data not shown).

Polarisation Transfer

Here we have shown that not only the ^{13}C-NMR lines of aromatic carbon atoms of the BChl and BPhe cofactors gain intensity by photo-CIDNP, but also carbon atoms that are located near the aromatic system. The photo-CIDNP enhancement of the aliphatic carbon nuclei of the cofactors has not been observed in natural abundance samples. Therefore, this enhancement must be due to a nucleus-to-nucleus polarisation transfer. It has not yet been clarified whether such polarisation transfer is caused by Karplus-Fraenkel hyperfine interaction (Karplus and Fraenkel, 1961) or by an alternative route.

Also the carbon nuclei in a magnesium-bound histidine side chain gain photo-CIDNP enhancement. These lines have also been observed in natural abundance samples (Figure 1). The question arises by which mechanism the carbon atoms in the proximity of the aromatic system gain nuclear-spin polarisation. In order to explain the observation of nuclear polarisation of nitrogen atoms of histidine, an intermediate electron transfer to the axial histidine ligand of a BChl cofactor has been proposed (Soede-Huijbregts *et al*., 1998). On the other hand, there is some overlap between the p_z-orbitals of the BChl nitrogens and the τ-N atom of the axial histidine, which may enable a direct polarisation transfer between both π-systems. This also would be in line with the data and assignments by Zysmilich and McDermott (1996b), showing that the signal from the τ-nitrogen at 201 ppm weakens but does not vanish upon diluting the ^{15}N-label concentration. The signal of the π-nitrogen at 147 ppm, which is far from the BChl, vanishes completely. This agrees with

the weakness of the signals of the γ-carbon in our experiment with a natural abundance sample.

Despite the current lack of knowledge of the exact polarisation pathways, we could show that the dissipation of nuclear polarisation provides a tool for probing the ground state structure, not only of the photochemically active aromatic systems, but also for its surroundings. This observation may provide the chance to use tailored photochemically active molecules to explore surfaces and cavities of membrane proteins by MAS NMR.

Materials and Methods

Sample Preparation

RCs from *R. sphaeroides* R-26 were isolated by the procedure of Feher and Okamura (1978), while RCs from wild-type *R. sphaeroides* were isolated using the method of Feher and Okamura with slight modifications. The removal of Q_A was done by incubating the reaction centres at a concentration of 0.6 μM in 4% LDAO, 10 mM *o*-phenanthroline, 10 mM Tris buffer, pH 8.0, for 6 h at 26 °C, followed by washing on a DEAE column. The reaction centres were removed from the column by washing with 0.5 M NaCl in 10 mM Tris buffer, pH 8.0, containing 0.025% LDAO and 1 mM EDTA (Okamura *et al*., 1975). Quinone reduction in the RC was performed by addition of 75 mM sodium ascorbate followed by freezing under illumination with white light with the sample in the NMR probe in the magnet. Approximately 5 mg of the RC protein complex embedded in LDAO micelles was used for the NMR measurements. The [1,3,6,8,11,13,17,19-$^{13}C_8$]-BChl/Bphe-labelled RC (Figure 3) was obtained with an incorporation rate of ca 60% by growth of *R. sphaeroides* WT in a standard medium supplemented with 1.0 mM [4-^{13}C]-aminolevulinic acid·HCl ($COOHCH_2CH_2{}^{13}COCH_2NH_2$; 100 mg), which was purchased from Cambridge Isotope Laboratories (99% ^{13}C-enriched). Details of the labelling strategy will be published elsewhere (Schulten *et al.*, in preparation).

MAS-NMR Measurements

NMR experiments were performed with MSL-400 and DMX-400 NMR spectrometers (Bruker, Karlsruhe, Germany) equipped with a double-resonance magic angle spinning (MAS) probe operating at 396.5 MHz for ^{1}H and 99.7 MHz for ^{13}C. The sample was loaded into a 4- or 7-mm clear sapphire rotor and inserted into the MAS probe. ^{13}C MAS NMR spectra were obtained with a spinning frequency ν_r=4 or 5 kHz at a temperature of 220 K. At the start of the experiments, the sample was frozen slowly with liquid nitrogen-cooled bearing gas, using slow spinning of ν_r=600 Hz to ensure a homogeneous sample distribution against the rotor wall (Fischer *et al.*, 1992). To obtain spectra under illumination, the sample was continuously irradiated from the side of the spinning sapphire rotor. The light and dark spectra were collected with a Hahn echo pulse sequence and TPPM proton decoupling (Bennet *et al*., 1995). Typically, a recycle delay of 12 s was used. With the natural abundance samples, a total number of 24 000 scans per spectrum were collected over a period of 24 h. An exponential line broadening of 70 Hz was applied prior to Fourier transformation. With the [1,3,6,8,11,13,17,19-$^{13}C_8$]-BChl/Bphe-labelled sample, the 1-D light spectra were recorded within 10 minutes. For the 1-D light spectra, a line broadening of 25 Hz was used. All ^{13}C-MAS NMR spectra were referenced to the ^{13}COOH response of solid tyrosine·HCl at 172.1 ppm.

The light illumination set-up has been described elsewhere (Matysik *et al*., 2000a). An average value of about 50 photons per second per RC has been estimated for the light excitation intensity (Matysik *et al*., 2001). After improvements of the illumination set-up, an increase of light intensity of about 20% was reached.

Acknowledgements

The authors thank B.M.M. Joosten for the help in the purification of the RCs. The kind help of K. Erkelens, J.G. Hollander and F. Lefeber in the operation of the NMR spectrometers is acknowledged. J.M. acknowledges a Casimir-Ziegler award of the Academies of Sciences in Amsterdam and Düsseldorf. This work was financially supported by the PIONIER programme of the Chemical Sciences section of the Netherlands Organization for Scientific Research (NWO).

References

Alia, Matysik, J., Soede-Huijbregts, C., Baldus, M., Raap, J., Lugtenburg, J., Gast, P., van Gorkom, H.J., Hoff, A.J., and de Groot, H.J.M. (2001). Ultra high field MAS NMR dipolar correlation spectroscopy of histidine residues in light harvesting complex II from photosynthetic bacteria reveals partial internal charge transfer in the B850/his complex. J. Am. Chem. Soc. *123*, 4803 – 4809.

Bennet, A.E., Rienstra, C.M., Auger, M., Lakshmi, K.V., and Griffin, R.G. (1995). Heteronuclear decoupling in rotating solids. J. Chem. Phys. *103*, 6951 – 6958.

Bixon, M., Jortner, J., and Michel-Beyerle, M.E. (1993). The singlet-triplet splitting of the primary radical pair in the bacterial photosynthetic reaction center. Z. Phys. Chem. *180*, 193 – 208.

Blankenship, R.E., Schaafsma, T.J., and Parson W.W. (1977). Magnetic field effects on radical pair intermediates in bacterial photosynthesis. Biochim. Biophys. Acta *461*, 297 – 305.

Corvaja, C., Franco, L., Mazzoni, M., Maggini, M., Zordan, G., Menna, E., and Scorrano, G. (2000). CIDEP of fullerene C60 biradical bisadducts by interamolecular triplet-triplet quenching: a novel spin polarization mechanism for biradicals. Chem. Phys. Lett. *330*, 287 – 292.

Deisenhofer, J., Epp, O., Miki, K., Huber, R., and Michel, H. (1985). Structure of the protein subunits in the reaction centre of *Rhodopseudomonas viridis* at 3 Å resolution. Nature *318*, 618 – 624.

Feher, D., and Okamura, M.Y. (1978). Chemical composition and properties of reaction centers. In: The Photosynthetic Bacteria, R.K. Clayton and W.R. Sistrom, eds. (New York, USA: Plenum Press), pp. 349 – 378.

Fischer, M.R., de Groot, H.J.M, Raap, J., Winkel, C., Hoff, A.J., and Lugtenburg, J. (1992). ^{13}C magic angle spinning NMR study of the light-induced and temperature-dependent changes in *Rhodobacter sphaeroides* R26 reaction centers enriched in [4'-13C]-tyrosine. Biochemistry *31*, 11038 – 11049.

Hoff, A.J., Gast, P., and Romijn, J.C. (1977a). Time resolved ESR and chemically induced dynamic electron spin polarisation of the primary reaction in a reaction centre particle of *Rhodopeudomonas sphaeroides* wild type at low temperatures. FEBS Lett. *73*, 185 – 190.

Hoff, A.J., Rademaker, H., van Grondelle, R., and Duysens, L.N.M. (1977b). On the magnetic field dependence of the yield of the triplet state in reaction centres of photosynthetic bacteria. Biochim. Biophys. Acta *460*, 547 – 554.

Hoff, A.J. (1981). Magnetic field effects on photosynthetic reactions. Quart. Rev. Biophys. *14*, 599 – 665.

Hoff, A.J. (1984). Electron spin polarisation of photosynthetic reactants. Quart. Rev. Biophys. *17*, 153 – 282.

Hore, P. J., and Broadhurst, R. W. (1993). Photo-CIDNP of biopolymers. Progr. NMR Spectrosc. *25*, 345 – 402.

Jeschke, G. (1997). Electron-electron-nuclear three-spin mixing in spin-correlated radical pairs. J. Chem. Phys. *106*, 10072 – 10086.

Jeschke, G. (1998). A new mechanism for chemically induced dynamic nuclear polarisation in the solid state. J. Am. Chem. Soc. *120*, 4425 – 4429.

Kaptein, R. (1975). Chemically induced dynamic nuclear polarisation: theory and applications in mechanistic chemistry. In: Advances in Free-Radical Chemistry, Vol. 5, G.H. Williams, ed. (New York, USA: Academic Press), pp. 319 – 380.

Kaptein, R. (1977). Introduction into chemically induced magnetic polarisation. In: Chemically Induced Magnetic Polarisation, L.T. Muss, P.W. Atkins, K.A. McLauchlan, and J.B. Pederson, eds. (Dordrecht, The Netherlands: Reidel), pp. 1 – 16.

Karplus, M., and Fraenkel, G.K. (1961). Theoretical interpretation of carbon-13 hyperfine interactions in electron spin resonance spectra. J. Chem. Phys. *35*, 1312 – 1323.

Kothe, G., Bechthold, M., Link, G., Ohmes, E., and Weidner J.U. (1998). Pulsed EPR detection of light-generated nuclear coherences in photosynthetic reaction centers. Chem. Phys. Lett. *283*, 51 – 60.

Matysik, J., Alia, Hollander, J.G., Egorova-Zachernyuk, T., Gast, P., and de Groot, H.J.M. (2000a). Sample illumination and photo-CIDNP in a magic-angle spinning NMR probe. Indian J. Biochem. Biophys. *37*, 418 – 423.

Matysik, J., Alia, Gast, P., van Gorkom, H.J., Hoff, A.J., and de Groot, H.J.M. (2000b). Photochemically induced dynamic nuclear polarisation in reaction centres of photosystem II observed by ^{13}C-solid-state NMR reveals a strongly asymmetric electronic structure of the P680$^{\bullet+}$ primary donor chlorophyll. Proc. Natl. Acad. Sci. USA *97*, 9865 – 9870.

Matysik, J., Alia, Gast, P., Lugtenburg, J., Hoff, A.J., and de Groot, H.J.M. (2001). Photochemically induced dynamic nuclear polarisation in bacterial photosynthetic reaction centres observed by ^{13}C solid-state NMR. In: The Future of Solid-State NMR, S. Kiihne and H.J.M. de Groot, eds. (Dordrecht, The Netherlands: Kluwer Academic Publishers), pp. 215 – 225.

McDermott, A., Zysmilich, M.G., and Polenova, T. (1998). Solid state NMR studies of photoinduced polarisation in photosynthetic reaction centres: mechanism and simulations. Solid State Nucl. Mag. Res. *11*, 21 – 47.

Okamura, M.Y., Isaacson, R.A., and Feher, G. (1975). Primary acceptor in bacterial photosynthesis: Obligatory role of ubiquinone in photoactive reaction centres. Proc. Natl. Acad. Sci. USA *72*, 3491 – 3495.

Polenova, T., and McDermott, A.E. (1999). A coherent mixing mechanism explains the photoinduced nuclear polarisation in photosynthetic reaction centers. J. Phys. Chem. B *103*, 535 – 548.

Soede-Huijbregts, C., Cappon, J.J., Boender, G.J., Raap, J., Gast, P., Hoff, A.J., Lugtenburg, J., and de Groot, H.J.M. (1998). ^{15}N MAS NMR spectroscopy of [π-15N] and [τ-15N] histidine labelled bacterial reaction centres. In: Photosynthesis, Mechanisms and Effects, Vol. 2, G. Garab, ed. (Dordrecht, The Netherlands: Kluwer Academic Publishers), pp. 759 – 762.

Van den Heuvel, D.J., Schmidt, J., and Wenckebach, W.T. (1994). Polarizing proton spins by electron-spin locking of photo-excited triplet state molecules. Chem. Phys. *187*, 365 – 372.

Weber, S., Berthold, T., Ohmes, E., Thurnauer, M.C., Norris, J.C., and Kothe G. (1996). Nuclear coherences in photosynthetic reaction centers following light excitation. Appl. Magn. Reson. *11*, 461 – 469.

Wegner, M., Fischer, H., Koeberg, M., Verhoeven, J.W., Oliver, A.M., and Paddon-Row, M.N. (1999). Time-resolved CIDNP from photochemically generated radical ion pairs in rigid bichromophoric systems. Chem. Phys. *242*, 227 – 234.

Wegner, M., Fischer, H., Grosse, S., Vieth, H.M., Oliver, A.M., and Paddow-Row, M.N. (2001). Field dependent CIDNP from photochemically generated radical ion pairs in rigid bichromophoric systems. Chem. Phys. *264*, 341 – 353.

Zysmilich, M.G., and McDermott, A.E. (1994). Photochemically induced dynamic nuclear-polarisation in the solid-state N-15 spectra of reaction centres from photosynthetic bacteria *Rhodobacter sphaeroides* R-26. J. Am. Chem. Soc. *116*, 8362 – 8363.

Zysmilich, M.G., and McDermott, A.E. (1996a). Natural abundance solid-state carbon NMR studies of photosynthetic reaction centers with photoinduced polarisation. Proc. Natl. Acad. Sci. USA *93*, 6857 – 6860.

Zysmilich, M.G., and McDermott, A.E. (1996b). A photochemically induced nuclear spin polarisation in bacterial photosynthetic reaction centers: assignments of the N-15 SSNMR spectra. J. Am. Chem. Soc. *118*, 5867 – 5873.

Received April 25, 2001; accepted July 3, 2001